Transport and diffusion on crystalline surfaces under external forces

2005 New J. Phys. 7 29

(http://iopscience.iop.org/1367-2630/7/1/029)

New Journal of Physics
The open–access journal for physics

Transport and diffusion on crystalline surfaces under external forces

Katja Lindenberg[1], **A M Lacasta**[1,2], **J M Sancho**[1,3] **and A H Romero**[1,4]

[1] Department of Chemistry and Biochemistry 0340, and Institute for Nonlinear Science, University of California, San Diego, La Jolla, CA 92093-0340, USA
[2] Departament de Física Aplicada, Universitat Politècnica de Catalunya, Avinguda Doctor Marañon 44, E-08028 Barcelona, Spain
[3] Departament d'Estructura i Constituents de la Matèria, Facultat de Física, Universitat de Barcelona, Diagonal 647, E-08028 Barcelona, Spain
[4] Advanced Materials Department, IPICyT, Apartado Postal 3-74 Tangamanga, 78231 San Luis Potosí, SLP, México
E-mail: klindenberg@ucsd.edu

New Journal of Physics **7** (2005) 29
Received 24 September 2004
Published 31 January 2005
Online at http://www.njp.org/
doi:10.1088/1367-2630/7/1/029

Abstract. We present a numerical study of classical particles obeying a Langevin equation and moving on a solid crystalline surface under an external force that may either be constant or modulated by periodic oscillations. We focus on the particle drift velocity and diffusion. The roles of friction and equilibrium thermal fluctuations are studied for two nonlinear dynamical regimes corresponding to low and to high but finite friction. We identify a number of resonances and antiresonances, and provide phenomenological interpretations of the observed behaviour.

PII: S1367-2630(05)86969-1

Contents

1. Introduction

The transport and diffusion properties of Brownian particles continues to attract enormous interest and activity even though a century has passed since the appearance of the famous seminal work of Einstein on the subject [1]. The motion of atoms, vacancies, excitations, molecules and clusters of molecules on surfaces (crystalline or disordered) is an active area of research due to its theoretical interest and technological relevance. One of the more recent research foci concerns the experimental and numerical observation that even for large clusters of molecules, long jumps spanning many lattice sites may in some cases be the dominant contributor to the motion [2]–[7]. This observation has elicited considerable theoretical interest [8]–[10], because it is at odds with the traditional models that rely on the notion that molecules move by making an occasional jump from one potential minimum to a nearest neighbouring one via a thermal activation process [11]. In a recent work [12], we have suggested that these long, even Lévy-like, motions can be described by ordinary Langevin dynamics in the low-friction regime and do not require the input of any extraordinary assumptions about the driving fluctuations. Since most of the theoretical work in the past has focused (usually for mathematical simplicity) on the overdamped problem, this possibility had not been fully explored.

A related avenue of extensive investigation has dealt with the transport properties of particles in a symmetric periodic potential subject not only to thermal effects but also to external forces. This interest lies in the extensive range of important physical applications that include Josephson junctions [13, 14], superionic conductors [15], adsorbates on crystal surfaces [16], colloidal spheres [17] and polymers diffusing at interfaces [18] among many others [19]. A constant external force produces a so-called 'tilted potential' or 'tilted washboard potential', and the further addition of a periodic force gives rise to the 'rocked tilted potential'. This is the problem considered in this paper. While there is an extensive literature on the subject (see e.g., [20] and references therein), among which is the excellent classic chapter in [19], there are still a number of interesting issues that seem not to have been addressed. Here we deal only with symmetric surface potentials, that is, we do not discuss the enormously important and prolific related area of transport in the so-called Brownian motors with ratchet (asymmetric) potentials.

The motion of a collection of noninteracting classical Brownian particles of mass m in this scenario is described by a standard Langevin equation in a two-dimensional periodic potential

$V(x, y)$ of characteristic length scale λ driven by an external force $\boldsymbol{F}(t)$ in the presence of thermal noise and the associated dissipation. The equations of motion for the components (x, y) of the position vector $\boldsymbol{r}$ are

$$\begin{aligned} m\ddot{x} &= -\frac{\partial}{\partial x}V\left(\frac{x}{\lambda}, \frac{y}{\lambda}\right) - \mu\dot{x} + F_x(t) + \xi_x(t), \\ m\ddot{y} &= -\frac{\partial}{\partial y}V\left(\frac{x}{\lambda}, \frac{y}{\lambda}\right) - \mu\dot{y} + F_y(t) + \xi_y(t), \end{aligned} \tag{1}$$

where an overdot denotes a derivative with respect to t. The generalization to distinct length scales λ_x and λ_y is straightforward. The parameter μ is the phenomenological coefficient of friction, and the $\xi_i(t)$ are mutually uncorrelated white (thermal) noises that obey the equilibrium fluctuation–dissipation relation,

$$\langle \xi_i(t)\xi_j(t')\rangle = 2\mu k_B T\, \delta_{ij}\, \delta(t - t'). \tag{2}$$

We choose the standard separable periodic potential,

$$V(x, y) = \frac{V_0}{2}\left[\cos\left(\frac{2\pi x}{\lambda}\right) + \cos\left(\frac{2\pi y}{\lambda}\right)\right], \tag{3}$$

which has maxima at positions $(n\lambda, m\lambda)$ and minima at $((n + \frac{1}{2})\lambda, (m + \frac{1}{2})\lambda)$, where n and m are integers. The barrier height at the saddle points is V_0, which we set to unity. The external force $\boldsymbol{F}(t)$ has a 'dc' constant component $\boldsymbol{F}_0$ and may also include an 'ac' periodic component:

$$\boldsymbol{F}(t) = \boldsymbol{F}_0 + \boldsymbol{F}_1 \cos(\omega t). \tag{4}$$

We stress that the model (1) is a 'standard' Brownian motion model. It relies on well-established ideas of statistical mechanics. The random forces are normal thermal fluctuations, Gaussian and δ-correlated, and the dissipative forces that accompany the fluctuations are constructed so as to ensure thermal equilibrium.

This model and others closely related to it have been studied extensively. In organizing the available information, it is useful to note a few salient points. Firstly, in the absence of a 'dc' force, a particle does not acquire a systematic velocity (i.e., the trajectories are 'locked'), but the distribution of positions does spread in phase space, i.e., while the average displacement $\langle \boldsymbol{r}\rangle$ away from the origin is zero, the mean-square displacement $\langle \boldsymbol{r}^2\rangle$ grows with time and one typically studies the nature of this growth in different parameter regimes. In the presence of a 'dc' force, on the other hand, the particle may acquire a nonzero velocity and then it becomes interesting to study the particle mobility related to the way that $\langle \boldsymbol{r}\rangle$ grows with time as well as the dispersion around this growth. The nature of the transition from 'locked' to 'running' solutions is at the core of the questions one deals with in the presence of a force. Secondly, it is important to realize that noise plays a fundamental role in the dynamics. Thus, for example, if the system finds itself in a state that would be metastable or even stable in the absence of noise ('locked'), the smallest amount of noise may cause a transition to a 'running' solution. Thus, it may be that the system is relatively insensitive to the magnitude of the noise (i.e., to the value of the temperature), but enormously sensitive to its very presence, the zero-noise case being a singular point. Thirdly, perhaps the most fundamental distinction to be made in these studies is the value

of the friction, because the system behaves profoundly differently in the overdamped limit (the most extensively explored case) than in the limit of low friction (a case far less well understood) [10, 20, 21].

The single most comprehensive study of this system that led to a subsequent outburst of interest was that of Risken [19]. His detailed studies of mobilities, distribution functions, transitions between different solutions, susceptibilities, eigenvalues and eigenfunctions and many other features in all parameter regimes provide a treasure trove of information. The literature on the tilted washboard potential that followed has focused mostly on the one-dimensional overdamped problem, where the double time derivative (inertial) term in the equation of motion is omitted. Here, there has been considerable focus on the enhancement of diffusion in the transition regime between locked and running solutions [21]–[24]. A direct experimental verification of some of the features of the transition has been implemented in [25]. The enhancement of diffusion in the one-dimensional underdamped problem, along with questions specifically associated with low damping such as resonance properties and nonexponential jump-length distributions have been addressed in [21, 26, 27]. The effect of adding a periodic force to the one-dimensional tilted potential in the overdamped case leads to further enhancement of the diffusion [28, 29] and to other nonlinear responses [30]. In the underdamped regime there are, in addition to the enhancement of diffusion, synchronization phenomena due to inertia [20, 31].

In spite of this extensive literature, we have not found a systematic study in which the mean velocity and the diffusion of the particles as a function of the different parameters of the force are studied together and their variations correlated with one another. More explicitly, our aim here is to study the velocity and diffusion of Brownian particles in a periodic potential under an external field with a 'dc' and also with an additional 'ac' component. Here we focus on a 'dc' force along a symmetry axis of the system (e.g., in the x-direction of our simple square lattice) and an oscillatory component along the same direction. This problem is effectively one dimensional. Although we could have posed a one-dimensional equation for this paper from the outset, this work is part of a broader program in which the bi-dimensionality is essential in the absence of forces [12] and also when the forces are not along a symmetry direction and/or parallel to one another [32]. In particular, we focus on the role of the *friction parameter*. Thus, while this problem has been extensively studied in the overdamped limit, as outlined above, we have found two important reasons for our effort: (1) we find that there is a considerable difference in the behaviour of the system with finite friction (even if large) than is found in the usual scenario of the asymptotic overdamped-limit case; that is, the large friction case is not universally represented by the overdamped limit; (2) The low-friction regime, which has not been explored nearly as much [19]–[21], presents a richer phenomenology.

The observables of interest to us, the average velocity and diffusion, are defined as follows:

$$v \equiv \lim_{t\to\infty} \frac{\langle x(t)\rangle}{t}, \tag{5}$$

$$D \equiv \lim_{t\to\infty} \frac{[x(t) - \langle x(t)\rangle]^2}{2t}. \tag{6}$$

The brackets $\langle\cdot\rangle$ indicate an ensemble average over many particles that includes an average over initial conditions and over noise realizations.

One of the challenges of studying a system described by several parameters is to place oneself in the parameter regime in which the interesting effects are observed. Consider, for

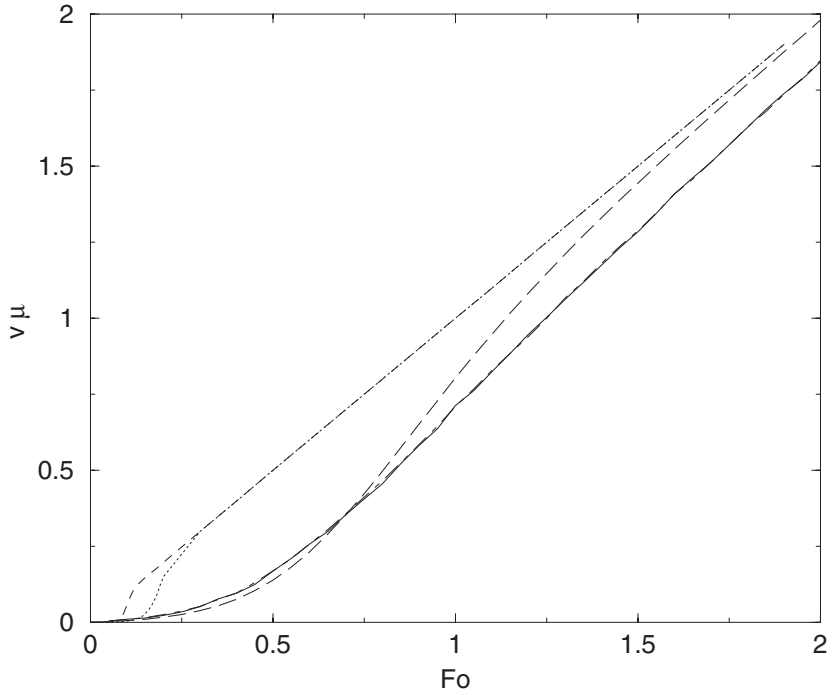

Figure 1. Average velocity of the Brownian particles for scaled temperature $\varepsilon = 0.2$ and various values of the friction coefficient. From left to right: $\mu = 0.05, 0.1, 1, 4$ and 5 (the latter two are indistinguishable on this scale). Of particular interest is the transition regime in each curve.

example, our system with a 'dc' external force $\boldsymbol{F}_0$ along the x-direction and with no oscillating component. Throughout this paper we set $\lambda = 4$, the value also used in our earlier work [12]. We set the dimensionless temperature at $\varepsilon \equiv k_B T/V_0 = 0.2$, a value that we often use in our simulations (although later we also study the effects on our results by varying the temperature). This ratio must be sufficiently small for the particle to recognize that it faces potential barriers, but sufficiently large for the particle to be able to overcome these barriers even in the absence of an external force in a reasonable simulation time. If the external force is zero, then the average velocity is zero. If the external force is very small, regardless of the friction coefficient, the average velocity is still zero or almost zero. On the other hand, if the external force is very large, the displacement of the particle grows linearly with time because the particle moves essentially ballistically as a free particle. The limiting velocity is $v = F_0/\mu$, where F_0 is the magnitude of the force. This result can be easily calculated from the equation of motion for a free particle under a constant force. These behaviours are illustrated in figure 1, where we show the velocity as a function of the force for the various values of the friction coefficient. A noteworthy point at the high-force limit is the following. Since we are plotting $v\mu$ on the vertical axis, all the velocity curves should converge to the value $v\mu = F_0$. We see that the low-friction curves do so quite early, but the high-friction curves appear not to. In fact, with increasing force all of them eventually converge to the single line. This is noteworthy because a calculation in the overdamped limit, where the inertial term is dropped and F_0 is finite, will not give the same result, but will instead give $v\mu = cF_0$, where c is a constant different from unity (it is the constant corresponding to the values seen within the range of the figure). One must therefore be cautious about overinterpreting

the results obtained when the inertial term is simply dropped from the equations of motion.

The interesting regimes for study are certainly neither the very small-force regime (where the particles are primarily in 'locked' states) nor the very large-force regime (where the 'running' solutions are no longer affected by the surface potential), but those intermediate regimes where the response of the system to the force is distinctly nonlinear. In the nonlinear regime, we expect interesting behaviour not only of the average particle velocity but also of the diffusion coefficient. This expectation is tied to the notion that in some sense the diffusion coefficient is a measure of the variation of the average velocity with F_0 (it is exactly this in the linear-response regime for a free particle, where $D = k_B T \mathrm{d}\langle v\rangle/\mathrm{d}F_0$) [21]. This expectation can be thought of as a generalization of the well-known Einstein relation $D = k_B T/\mu$ [1].

In order to locate these nonlinear regimes, we have performed a preliminary exploration of the mean velocity as a function of a constant force along the x-axis for different values of the friction. These results are shown in figure 1 where we can see linear zones with clearly nonlinear ones located at $F_0 \sim 0.1$ for the lowest friction curve and at $F_0 \sim 0.78$ for high friction. The interesting range of values of the external force is clearly friction-dependent, and we will choose F_0 accordingly in later sections. It is also clear from the figure that the increase in the velocity from zero to F_0/μ is very steep in the case of low friction ($\mu = 0.05, 0.1$), that is, the variation from locked to essentially free behaviour occurs over a very narrow-force regime, while in the high-friction regime ($\mu \gtrsim 1$) the rise is far more gradual.

The mechanisms for 'unlocking' a 'locked' state at high friction and at low friction are known to be very different [19], and the differences observed in the figure reflect this. In the high-friction case, the unlocking occurs when the tilt is sufficiently large for the minima of the potential to disappear; the transition thus occurs when the minima become marginally stable states, and is insensitive to the value of the friction (see the solid curve in figure 2; this description is appropriate in the strictly overdamped limit. When damping is high but not infinite, the transition occurs a bit before the state of marginal stability at a value of the force that exhibits a mild dependence on friction, see below). The running state thus essentially sets in when there are no potential barriers. In the low-friction case, the particles have inertia and can therefore escape the potential wells into a running state even when there are potential minima (see the dotted curve in figure 2). However, the depth of the well where this becomes possible is sensitively dependent on the friction, since it involves a balance between the loss of energy due to friction and the gain in kinetic energy due to the external force. This explains, among other features, why the transition sets in sooner and more strongly in the low-friction case than in the high-friction case. The $\mu = 1$ curve in figure 1 is exhibited as an intermediate case: the rise of the velocity from zero is similar to that of the high-friction cases but the approach to the asymptotic value is more rapid and similar to the low-friction cases. In our analysis, we choose the value $\mu = 0.05$ as a typical low friction and $\mu = 5$ as a typical high (but finite) friction.

The paper is organized as follows. In section 2, we explore the velocity and diffusion coefficient for the tilted washboard potential system in the low-friction regime, as a function of the friction and temperature. Here we also investigate the effects of introducing an oscillatory force parallel to the 'dc' external force. In section 3, we explore the velocity and diffusion coefficient for the same system but in the high-friction regime. Again, we also comment on the effects of an added oscillatory force. We find interesting resonance as well as antiresonance effects caused by the oscillatory component. A summary and some topics for future work are discussed in section 4.

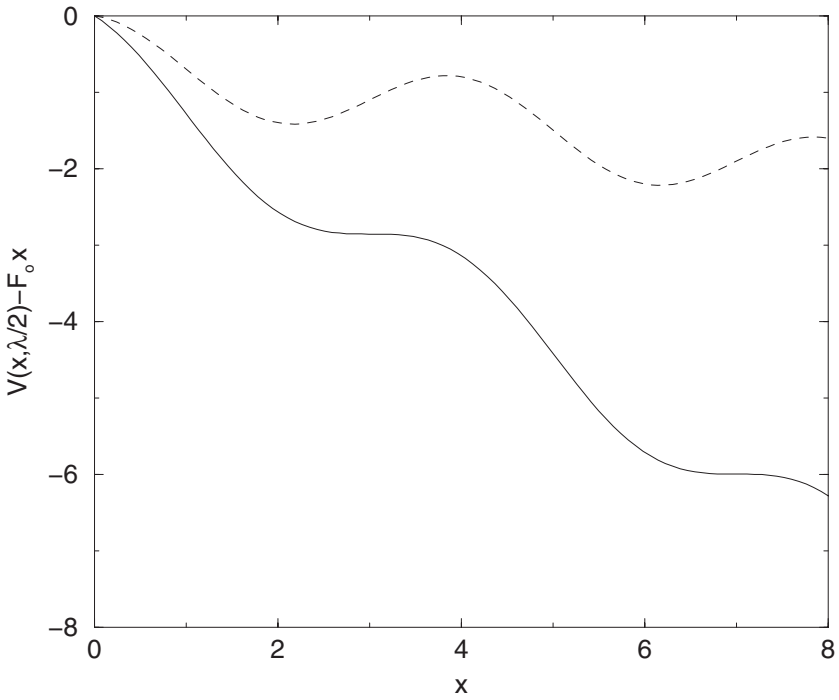

Figure 2. Tilted potential along the x-direction for $y = \lambda/2$ and different forces F_0. The dotted curve is for a small force, so while the potential is tilted it still exhibits clear maxima and minima. The solid curve is for the force that leads to marginal stability.

2. Low-friction regime

In this section, we consider the transport and diffusion properties of our particles on a periodic surface subject to an external force F_0 along the x-direction. In section 2.1, we apply a constant force and study the response as the force, friction and the temperature are varied. In section 2.2, we add an oscillatory force and consider the dependence of the response on frequency.

2.1. Constant external force

In the top panel of figure 3, we repeat an expanded view of the velocity versus F_0 curves of figure 1 in the low-friction regime, adding one more curve for $\mu = 0.3$. The lower panel shows the associated diffusion coefficient. To appreciate the differences in the magnitudes of these quantities for different friction coefficients it should be noted that in figure 3 both v and D have been multiplied by μ on the vertical axes.

As noted earlier, at very low friction the increase of the velocity with applied force F_0 occurs rather abruptly and reaches the large-force value $v = F_0/\mu$ over a narrow range of forces. In this narrow range, the diffusion coefficient achieves a maximum that is more pronounced for lower damping. The abrupt increase in the velocity versus F_0 has been described in some detail in [19, 21], and involves dynamical transitions between 'locked' and 'running' states that lead to a finite average velocity not yet equal to the velocity of a fully running solution. Indeed, at extremely low temperatures, this transition becomes increasingly abrupt, as the transition takes place at an increasingly specific value of the force. An interesting discussion of the discontinuous role of

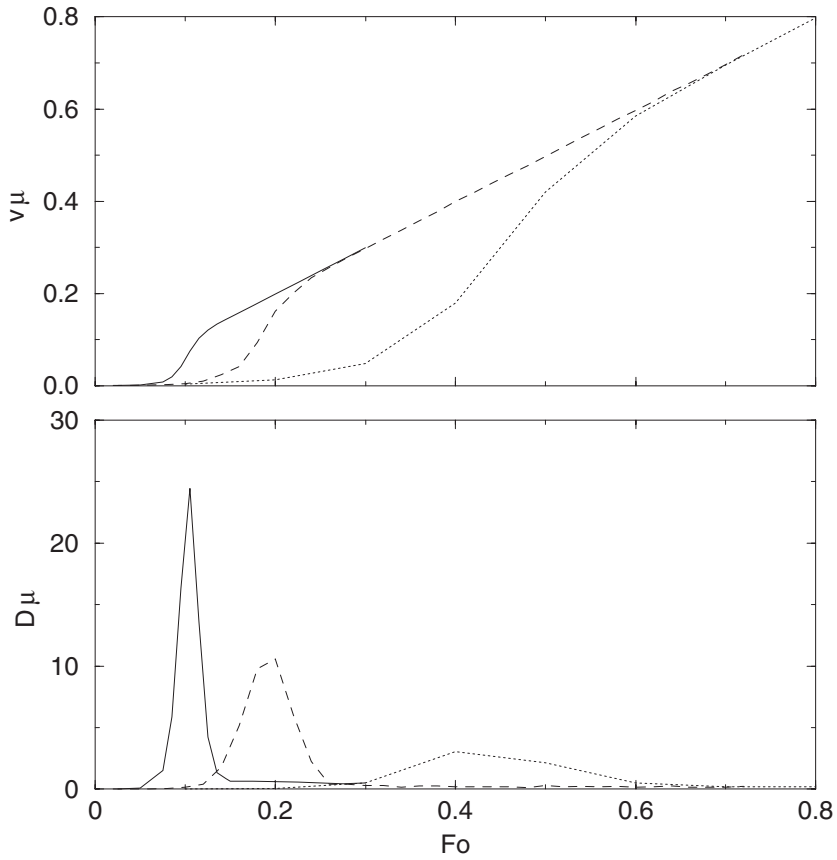

Figure 3. Mean velocity (top) and diffusion coefficient (bottom) versus F_0 for different values of the friction coefficient in the low-friction regime: $\mu = 0.05$ (——), $\mu = 0.1$ (- - - -) and $\mu = 0.3$ (· · · · · ·). The scaled temperature is $\varepsilon = 0.2$.

temperature in this regime (i.e., the difference between the behaviour at $T = 0$ and in the limit $T \to 0$) can also be found in [19, 21].

The diffusion coefficient is observed to peak in this regime. A typical particle trajectory moves randomly from locked to running back to locked, and so on. During a locked interval the velocity is zero, and diffusion around zero velocity may be small. During a running interval the velocity is not zero, and again the diffusion around the nonzero velocity may be small. As a result, the apparent diffusion about the average velocity v may be large, somewhat artificial, because this average velocity is not the most probable velocity of a particle. In other words, in this regime the velocity distribution is bimodal rather than unimodal about the average velocity [19, 21], and the calculated D is the full width of this bimodal distribution and not reflective of the width of each of the two modes. Note that the increased diffusion is consistent with the linear response theory result for a free particle that associates D with v through the derivative relation $D = k_B T \, \mathrm{d}v/\mathrm{d}F$. Our particle is neither free, nor is the force in the transition region particularly small, but nevertheless large diffusion is associated with a steep slope of velocity versus F_0 that comes about here because of the switching between different velocities. With increasing friction the transition region moves to higher forces and becomes less abrupt. The associated maximum of the diffusion coefficient then also moves to higher forces and becomes less pronounced.

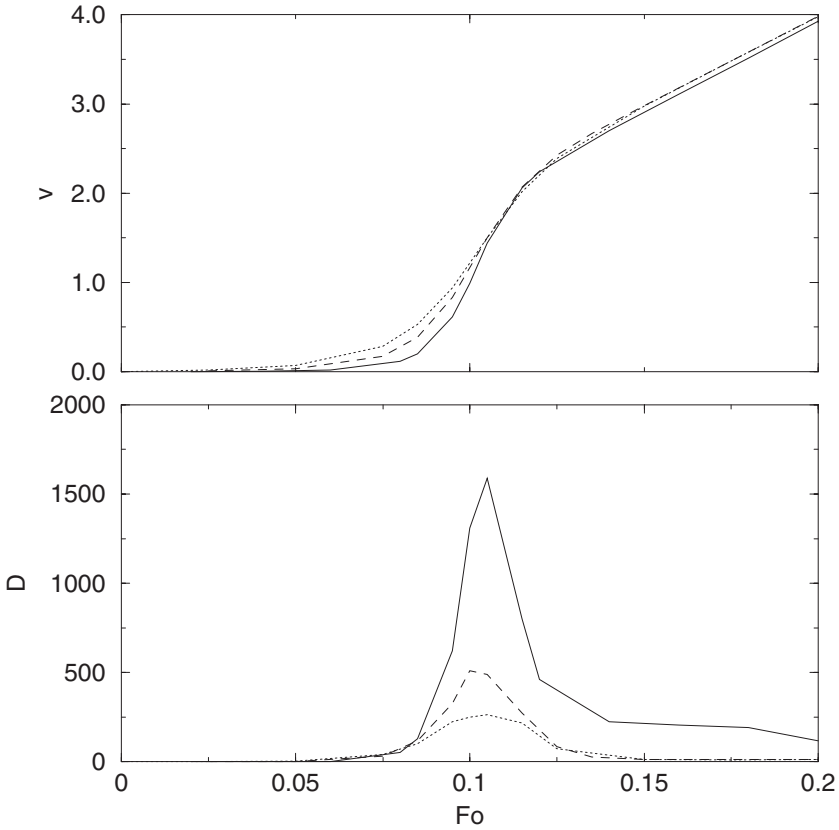

Figure 4. Mean velocity (upper panel) and diffusion (lower panel) versus F_0 for three values of the temperature: $\varepsilon = 0.15$ (——), $\varepsilon = 0.20$ (- - - -) and $\varepsilon = 0.25$ (dotted curve). The friction coefficient is fixed at $\mu = 0.05$.

The effect of changes in temperature on this system has received less attention. In the top panel of figure 4, we present the velocity versus F_0 curves for three values of the temperature for a system with friction coefficient $\mu = 0.05$, the lowest friction in figures 1 and 3. The lower panel again shows the associated diffusion coefficient for each of the three temperatures. The principal effect on the velocity by lowering the temperature is to sharpen the transition region, essentially without moving its location. The centre of the transition region, regardless of temperature, is located near the value of F_0, which defines the abrupt transition as temperature goes to zero. However, the effect on the diffusion coefficient is far more pronounced. While the location of the peak is essentially temperature independent, as we would expect from the fact that the velocity transition remains localized around the same value of the force, the peak grows with decreasing temperature, that is, diffusion is stronger as temperature decreases, again consistent with the sharpening of the velocity transition. This behaviour is also consistent with our earlier description of the diffusion in the switching region between locked and running states.

A plot of the maximum diffusion as a function of the temperature reveals the strongly nonlinear dependence

$$D_{\max} \sim T^{-3.5}, \tag{7}$$

that is, the diffusion coefficient seems to grow without bound as the temperature is lowered. Note that, if one were to argue for the validity of the linear response form $D = k_B T \, \mathrm{d}v/\mathrm{d}F_0$

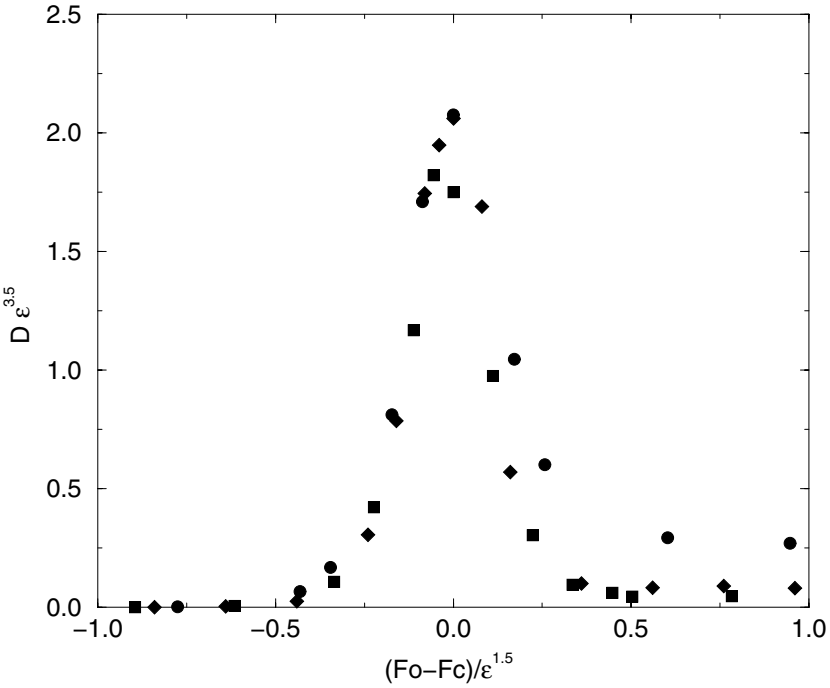

Figure 5. Scaled diffusion in the low-friction regime ($\mu = 0.05$) for various temperatures. ●, $\varepsilon = 0.15$; ■, $\varepsilon = 0.21$; and ◆, $\varepsilon = 0.25$.

even though the force at maximum diffusion is neither extremely small nor extremely large, the strongly nonanalytic dependence (7) indicates a strong temperature dependence of $\mathrm{d}v/\mathrm{d}F_0$. An interesting scaling behaviour (inspired by results in the high-damping regime, cf below) is observed if we plot the product $\varepsilon^{3.5}D$ as a function of $(F_0 - F_c)/\varepsilon^{1.5}$, as done in figure 5. Here F_c is the force at which the diffusion coefficient is a maximum, $F_c \sim 0.1$ for $\mu = 0.05$. With this scaling, all the curves in the bottom panel of figure 4 collapse onto the same curve. We stress that the exponents 3.5 and 1.5 of ε are simply numerical fits (and not necessarily the very best ε values), although the divergent increase of D with decreasing temperature is supported by the simulations for the temperatures studied. In any case, the result (7) as well as the scaling behaviour in figure 5 (or ones with even more accurate exponents) remains to be explained theoretically.

2.2. *Oscillatory external force*

In addition to the constant external force of magnitude F_0, we now consider the effect of an oscillatory force, as in equation (4), with $\boldsymbol{F}_1$ also along the x-direction. In this work, we fix the magnitude of the oscillatory force to be half the constant force component, $F_1 = F_0/2$. Variations of this amplitude will be considered elsewhere [32]. Since the force is oscillatory, it is interesting to explore the possibility of resonances caused by the resultant rocking of the potential. We note that the potential wells persist throughout the oscillations, i.e., the tilt produced by $F_0 + F_1 = 3F_0/2$ is still not enough to eliminate the extrema (cf figure 2).

In figure 6 we show the average velocity and diffusion coefficient as a function of the frequency ω of the oscillatory force for two values of the friction coefficient. The value of the

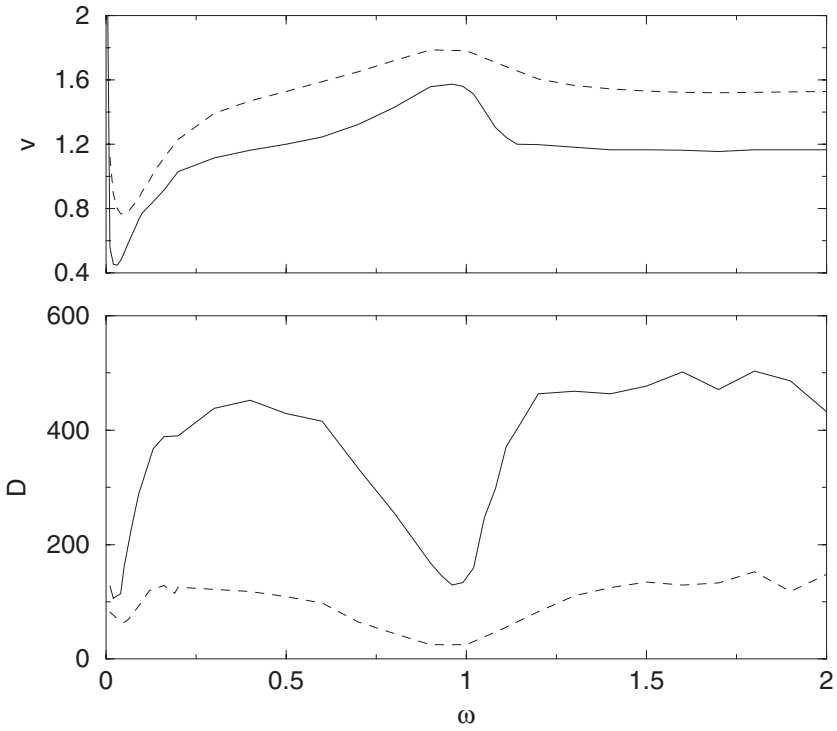

Figure 6. Average velocity (upper panel) and diffusion coefficient (lower panel) as a function of the frequency of the oscillatory force. ——, $\mu = 0.05$ and $F_0 = 0.1$; - - - -, $\mu = 0.1$ and $F_0 = 0.2$. The scaled temperature in both cases is $\varepsilon = 0.2$.

constant force F_0 and the amplitude of the oscillatory component $F_1 = F_0/2$ have been chosen differently for the two cases so as to focus on the F_0 regime of greatest sensitivity of the average velocity (keeping F_0 fixed would take us out of this regime for one or the other friction). The trend is clearly seen in the figure. There is a maximum in the average velocity and an associated minimum in the diffusion coefficient when the frequency of the oscillatory force matches with that of the potential wells ($\omega \approx 1$). One can imagine the particle oscillating back and forth in the tilted potential, with the oscillatory force pushing it along by further tilting of the potential even more favourably just as the particle reaches the next maximum. In our earlier picture of the bimodal distribution of velocities in this regime, the oscillatory force causes a decrease of the zero-velocity peak and an increase of the finite-velocity peak. As a result, at this point of resonance of the particle velocity, the width of the distribution also decreases, and this is seen in the pronounced decrease of the diffusion coefficient.

At very low frequencies we see a minimum in the velocity. We interpret this as a value of the frequency at which the rocking of the potential causes the particle to move forward for several periods, and then backward for a number of periods. The resulting average velocity is then significantly lowered. In the bimodal velocity distribution picture, the oscillatory force causes a decrease of the finite velocity peak and an increase of the zero velocity peak. As a result, at this point of antiresonance, the width of the distribution again decreases, and this, too, is seen as a decrease of the diffusion coefficient.

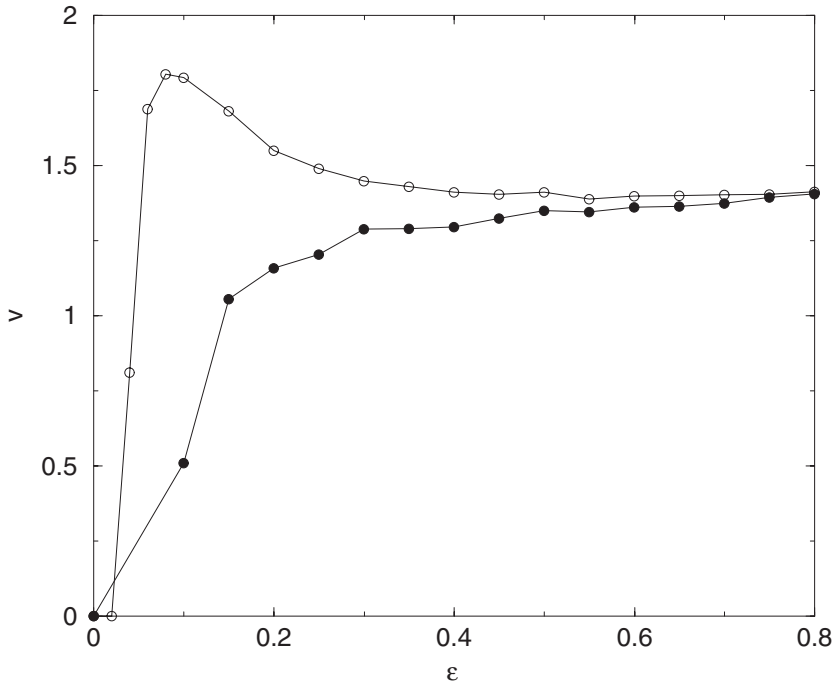

Figure 7. Mean velocity versus noise intensity with (○) and without (●) an oscillatory force component of unit frequency. The friction coefficient in both cases is $\mu = 0.05$, and the constant component of the external force is $F_0 = 0.1$. The amplitude of the oscillatory force is $F_1 = F_0/2 = 0.05$.

The other interesting behaviour to explore is the temperature dependence of the resonance observed in figure 7. We see that in the absence of an oscillatory component the average velocity simply increases monotonically with increasing noise. At sufficiently large values of the noise (not shown here), the average velocity asymptotes to the free-particle value F_0/μ. In the presence of an oscillatory component, there is an optimal value of the noise that leads to a maximum average velocity. We have not yet explored this behaviour beyond the observation of the existence of this maximum.

3. High-friction regime

3.1. Constant external force

When a constant external force of magnitude F_0 is applied in the x-direction at sufficiently high friction, the product $v\mu$ as a function of F_0 becomes virtually independent of μ. In particular, for $\mu \gtrsim 3$ the familiar overdamped dependence $v \sim 1/\mu$ is essentially exact. The diffusion coefficient exhibits a maximum in the region of greatest variation of v versus F_0 [22], once again confirming the earlier comments concerning the proportionality of D and $\mathrm{d}v/\mathrm{d}F_0$. While the velocity distribution in the high-friction regime is not expected to be bimodal, in this region of greatest variation there is a relatively large spread of possible velocities so that the width of the unimodal distribution is relatively large compared to its width at lower forces (essentially

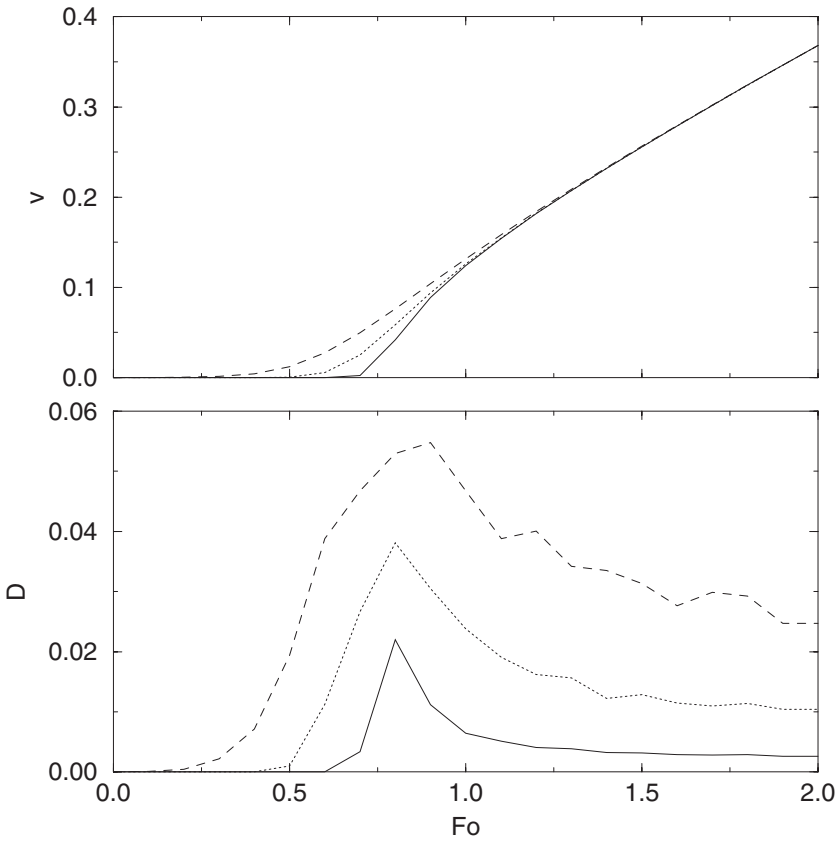

Figure 8. Average velocity (upper panel) and diffusion coefficient (lower panel) versus F_0 for three values of the temperature: $\varepsilon = 0.01$ (——), $\varepsilon = 0.04$ (· · · · · ·) and $\varepsilon = 0.1$ (- - - -). The friction coefficient is $\mu = 5$ in all three cases.

no motion) and at higher forces (essentially free-damped motion). Along with this behaviour, we determined that the product of the maximum of the diffusion coefficient and the friction, which occurs at $F_0 \sim 0.78$, is also virtually independent of μ, again consistent with the familiar dependence $D \sim 1/\mu$. The magnitude of this maximum rapidly decreases with increasing friction, that is, increasing the friction inhibits diffusion, as expected.

Temperature dependence of the average velocity and diffusion constant are illustrated in figure 8 [33]. This sequence should be compared with the corresponding low-friction results of figure 4. While the location of the maxima in the diffusion coefficient and the associated midpoint of greatest variation of the average velocity is rather insensitive to the noise, a number of important contrasts between the high- and low-friction cases are noteworthy. Firstly, the values of the velocities and the diffusion coefficients are of smaller magnitude in the high-friction regime. Secondly, the temperatures we are considering here are also much smaller than those in figure 4 because those high temperatures would produce an essentially constant value of the diffusion coefficient until one reaches much higher forces. In turn, higher forces would place us outside the regime of interest, which is that of greatest variation of the velocity with F_0. The most important contrast, though, is the fact that here the peak value of the diffusion coefficient increases with increasing temperature, whereas the behaviour was exactly opposite in the low-friction case. This reflects the fact that with increasing noise the region connecting the

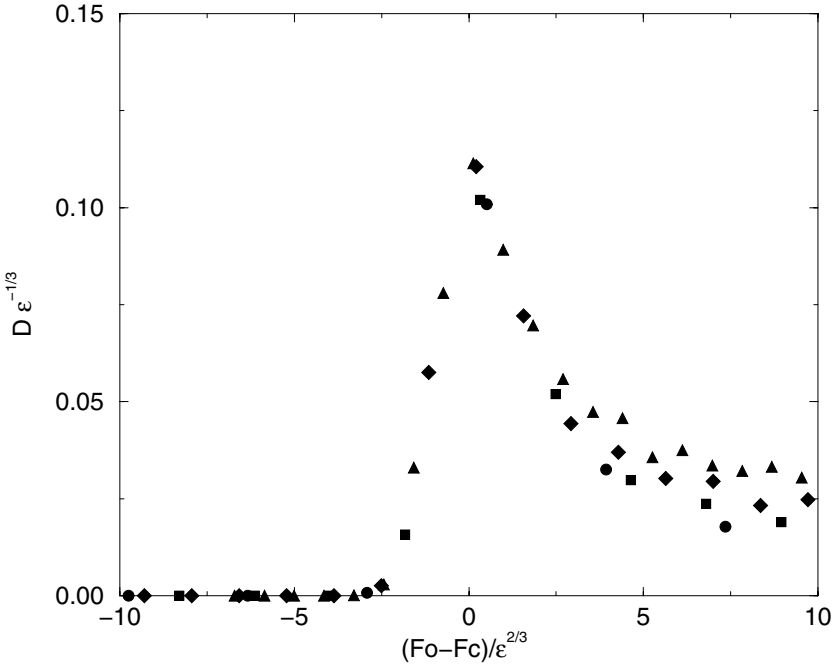

Figure 9. Scaled diffusion coefficient in the high-friction regime ($\mu = 5$) for various temperatures. ●, $\varepsilon = 0.005$; ■, $\varepsilon = 0.01$; ◇, $\varepsilon = 0.02$; and ▲, $\varepsilon = 0.04$.

low-force (essentially zero velocity) regime with the high-force (essentially linear) regime covers a wider range of forces with increasing temperature, which in turn translates to a (unimodal) velocity distribution that broadens with increasing temperature. This behaviour is summarized in the nonlinear dependence

$$D_{\max} \sim T^{1/3}, \tag{8}$$

obtained when we plot the maximum diffusion as a function of the temperature.

The temperature dependence (8) and the scaling behaviour of the diffusion coefficient shown in figure 9 can be obtained from the following scaling analysis [34] (for a more elaborate analysis see [22]) in the overdamped limit (which unfortunately seems to be difficult to generalize to the low-friction regime). In this extreme limit, we drop the inertial term $\ddot{x}$ in the first equation in equation (1) with $y = \lambda/2$, and expand the effective potential $V - F_0 x$ around the metastable point $x_c = 3\lambda/4 = 3$ and around the force of marginal stability $F_0 = F_c = V_0\pi/4$. The equation of motion for $X \equiv x - x_c$ (with $V_0 = 1$) then reduces to

$$\dot{X} = \frac{\pi}{2\mu}X^2 + \frac{1}{\mu}(F_0 - F_c) + \frac{1}{\mu}\xi(t), \tag{9}$$

exactly of the form considered in [34]. A rescaling of the variables with temperature as

$$X = \varepsilon^{1/3} z, \qquad t = \varepsilon^{-1/3} s \tag{10}$$

allows us to rewrite equation (9) as

$$\dot{z} = \frac{\pi}{2\mu} z^2 + \frac{1}{\mu}(F_0 - F_c)\varepsilon^{-2/3} + \eta(t), \tag{11}$$

where we now have the new noise with temperature-independent correlation function

$$\langle \eta(s)\eta(s') \rangle = 2\delta(s - s'). \tag{12}$$

The important point of this result is that one can explicitly see that the time scales of the dynamical variable X and the dependence on the force F_0 are determined by the parameter $\varepsilon^{-1/3}$ in equation (10) and the scaled variable $(F_0 - F_c)\varepsilon^{-2/3}$. The diffusion coefficient associated with the particle displacemet x in the absence of a force can be estimated as $D \sim \langle x_0^2 \rangle / t_0$, where x_0 is the size of a step between trapping events and t_0 is the time to perform this step. At high damping and low temperature, the diffusive events take the particle from one well to a nearest neighbouring well regardless of temperature. The time for this step, on the other hand, depends on temperature (becomes faster with increasing temperature) and according to the above argument scales with $\varepsilon^{-1/3}$. We thus conclude that

$$D \sim \varepsilon^{1/3} \phi \left((F_0 - F_c)\varepsilon^{-2/3} \right), \tag{13}$$

where ϕ is a scaling function. The upshot is that the diffusion coefficient scales with temperature as found in equation (8). Furthermore, a plot of $D\varepsilon^{-1/3}$ versus $(F_0 - F_c)\varepsilon^{-2/3}$ should lead to the collapse of all the curves in the lower panel of figure 8 onto a single curve. This is indeed observed in figure 9.

3.2. Oscillatory external force

Again, in addition to the constant external force we now add an oscillatory force whose magnitude is half that of the constant force and lies along the same direction. The average velocity as a function of the rocking frequency is shown in figure 10 for different values of the friction coefficient. This figure is the 'partner' of the upper panel of figure 6, but now for high friction. It presents a series of results for friction coefficients ranging from $\mu = 1$ to $\mu = 20$ in increments of $\Delta(1/\mu) = 0.05$. Note that since the system is highly damped, in order to obtain finite velocity solutions it is necessary that during at least part of the cycle the tilt be sufficiently strong that the extrema in the potential essentially disappear (cf figure 2 and related discussion).

There is a dramatic series of resonances and antiresonances in the behaviour of the average velocity as a function of the frequency of the oscillatory force. We envision the process as follows. In the portion of the oscillatory cycle where there are potential wells, the particle does not move away from the well in which it finds itself. As the tilt increases and the extrema disappear, the particle starts to roll down the incline. Suppose that just as the oscillatory motion begins to recover the potential extrema, the particle finds itself at a location just to the right of a maximum of the potential. The particle clearly rolls down to the next minimum, and does so more quickly than it would have in the absence of the extrema. The rocking motion has thus speeded up the particle. This corresponds to the resonances observed in figure 10. On the other hand, if at the moment when the oscillatory motion begins to recover the extrema of the potential, the particle finds itself just to the left of a maximum, the particle rolls back to the location of the previous minimum. Here the rocking motion has slowed down the particle, explaining the antiresonances observed in the figure. Note that the forward or backward pushes may occur at different locations

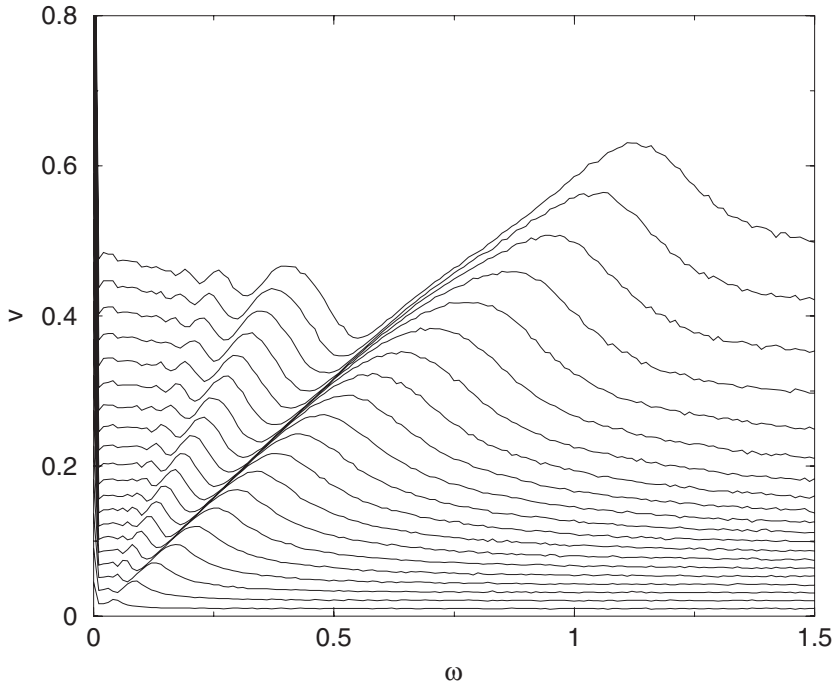

Figure 10. Average velocity as a function of the frequency of the oscillatory component of the force for various friction coefficients ranging from $\mu = 1$ (highest velocity curve) to $\mu = 20$ (lowest velocity curve) in increments of $\Delta(1/\mu) = 0.05$.

in the potential landscape depending on the rocking frequency, thus explaining the appearance of a series of maxima and minima with decreasing frequency.

One can estimate the location of these resonances and antiresonances (which clearly depend on the friction coefficient) as follows. A particle rolling down a slope in the absence of potential extrema gains a velocity of order $v = F_0/\mu$ as it covers the distance between what at a lower tilt would be a minimum to what would be a maximum. The distance covered in this journey is $\lambda/2$, from which one can calculate the time needed for the journey. If the inverse oscillation frequency matches this time, then instead of rolling onward the particle gets pulled back, yielding an antiresonance. The same effect is observed if the match occurs for a distance $3\lambda/2$, but the time involved is longer and hence the frequency lower. We have checked that this estimate leads to the correct behaviour by varying μ, but can only do so over a small range of μ for a given F_0 because the force F_0 at which each velocity curve in figure 10 is calculated is of course different. This can be seen in the different limiting velocities as a function of friction: at very high frequencies the velocity simply asymptotes to the value F_0/μ, which is different for each curve.

We interject a small but noteworthy point here about the behaviour of the velocity curves in the limit of zero frequency. One might naively expect this limiting velocity in each case to be simply that associated with the force $F_0 + F_1$, which should be higher than the high-frequency velocity associated with the force F_0. However, these curves, although calculated for long times, are nevertheless calculated for finite times (the length of time of the computation). The limits $t \to \infty$ and $\omega \to 0$ do not commute, and therefore we do not capture the strictly $\omega = 0$ behaviour.

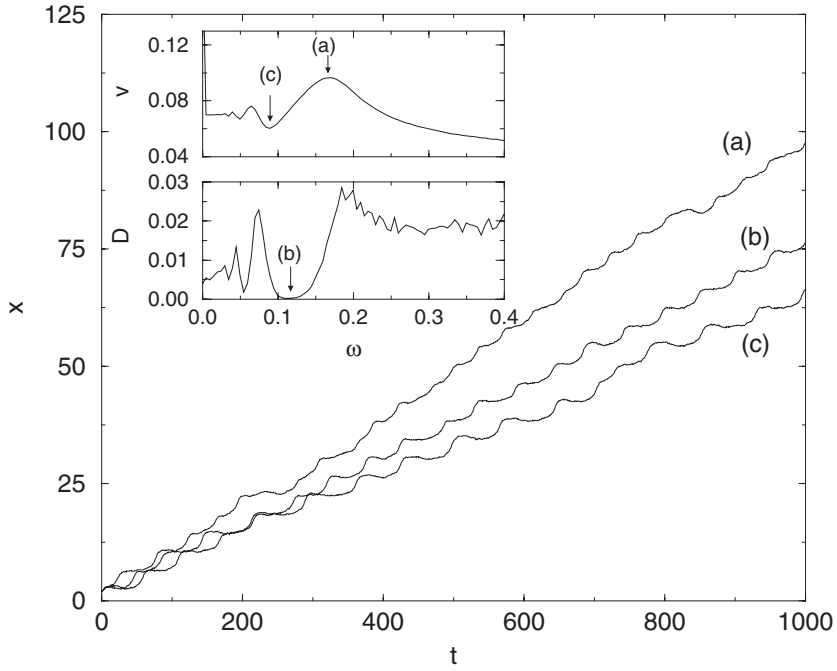

Figure 11. Three typical trajectories for $\mu = 5$, and insets of the velocity (upper) and the diffusion coefficient (lower) as a function of the frequency of the oscillatory component of the force. Trajectory (a) corresponds to a high velocity and an intermediate value of the diffusion coefficient. Trajectory (b) corresponds to an intermediate velocity and a very low diffusion coefficient. Trajectory (c) is associated with a low velocity and an intermediate diffusion coefficient. These trajectories and insets illustrate the difficulty of predicting these behaviours.

Finally, we comment on the fact that we have not shown our usual 'second panel' indicating the way in which the diffusion coefficient would vary with the frequency of the oscillatory force component, so as to ascertain whether the velocity resonances and antiresonances can be associated with high or low values of the diffusion. In figure 11, we illustrate why we have not done so. Here we illustrate the complicated nature of typical trajectories that have the virtue of showing the 'rolling forward' versus 'rolling backward' features discussed above. The figure shows three typical trajectories for $\mu = 5$. The upper panel in the inset shows the average velocity as a function of the frequency of the oscillatory force component, and the lower panel shows the associated diffusion coefficient. We have indicated three points on the curve and have labelled the trajectories accordingly. Thus, trajectory (a), which has the highest velocity, is associated with the high-velocity point (a) in the upper inset and with an intermediate value of the diffusion coefficient ($D = 0.016$). The variations of the velocity along the trajectory that give rise to the spread can be seen clearly, including places where there is actually a reversal of the velocity. Trajectory (b) is the most regular in the sense that it does not exhibit velocity reversals. The particle seems to move forward in a stop/advance/stop/advance regular sequence. The associated diffusion coefficient is very low, almost zero on the scale of the lower inset panel. Finally, trajectory (c) is quite irregular again, clearly showing velocity reversals. Here the diffusion coefficient rises again ($D = 0.007$). It is clearly difficult to predict these behaviours in detail, although the source of the variations is clear.

4. Conclusions

We have investigated the behaviour of an ensemble of particles in a two-dimensional potential subject to thermal fluctuations and external constant and oscillatory forces. Our description is based on ordinary Langevin dynamics and the focus has been on the effects of friction and temperature on the dynamics. While such systems have been of interest for several decades, our interest is motivated by the fact that (1) we have not found much work in the literature on correlated studies of the mean velocity and diffusion of the particles and their variations with system parameters; and (2) there is relatively little work in the literature that deals with inertial contributions. Such contributions are not only important at low damping, but they also affect the evolution of the system at high (but not infinite) damping.

Particle diffusion is in all cases greatest at constant values of the external force F_0 that lead to the fastest variation of the mean particle velocity v, that is, at values for which $\mathrm{d}v/\mathrm{d}F_0$ is greatest. We call these values F_c. At low friction the value of F_c decreases with decreasing friction, while the maximum of the diffusion coefficient increases rapidly with decreasing friction. We have provided qualitative explanations for this behaviour. The force F_c is insensitive to temperature, but the maximum of the diffusion coefficient is quite sensitive to temperature in a highly nonanalytic way ($D \sim T^{-3.5}$) for which we have no theoretical explanation. We have presented a scaling behaviour of the diffusion coefficient with temperature and force near F_c that needs to be explained. Addition of an oscillatory component leads to interesting resonances and antiresonances of the particle velocity as a function of oscillatory frequency, always accompanied by minima of the diffusion coefficient at those frequencies. Again, qualitative explanations for these results have been provided. A maximum of the mean particle velocity as a function of temperature in the presence of an oscillatory component of the force is also observed.

In the high-friction regime, the force F_c is insensitive to the value of the friction parameter. Now, contrary to the low-friction regime, the diffusion coefficient increases with increasing temperature ($D \sim T^{1/3}$). This dependence, as well as the scaling with the force near F_c, is described in terms of a theory of metastability first developed in [34] and confirmed here by numerical simulations. Finally, addition of an oscillatory component to the force led to a series of dramatic resonances and antiresonances in the particle velocity versus oscillatory frequency ω associated with where exactly the particle is located when the rocking motion of the potential reverses its tilt. While we understand this behaviour, the behaviour of the diffusion coefficient versus ω is far more complicated and difficult to predict in a systematic fashion.

Among the most interesting extensions of this work is the study of the effects of forces along different directions. The results of such a study will be presented elsewhere [32].

Acknowledgments

AML, JMS and AHR acknowledge the kind hospitality of the Department of Chemistry and Biochemistry at University of California at San Diego, where this work was initiated. This work was supported by the Engineering Research Program of the Office of Basic Energy Sciences at the U.S. Department of Energy under the grant no DE-FG03-86ER13606, by a grant from the University of California Institute for México and the United States (UC MEXUS) and the Consejo Nacional de Ciencia y Tecnología de México (CoNaCyT), and by the MCyT (Spain) under the project BFM2003-07850. AML acknowledges support from the Generalitat de Catalunya under the grant 2004BE00074. AHR acknowledges financial support from CONACyT–Mexico through the grant J-42647-F.

References

[1] Einstein A 1905 *Ann. Phys.* **17** 549
[2] Cowell Senft D and Ehrlich G 1995 *Phys. Rev. Lett.* **74** 294
Linderoth T R *et al* 1997 *Phys. Rev. Lett.* **78** 4978
Graham A P *et al* 1997 *Phys. Rev.* B **56** 10567
Oh S-M *et al* 2002 *Phys. Rev. Lett.* **88** 236102
[3] Luedtke W D and Landman U 1999 *Phys. Rev. Lett.* **82** 3835
[4] Wecksesser J, Barth J V, Cai C, Müller B and Kern K 1999 *Surf. Sci.* **431** 168
Weckesser J 2000 *PhD Thesis* Swiss Federal Institute of Technology, Laussane
[5] Schunack M, Linderoth T R, Rosei F, Laengsgaard E, Stendgaard I and Besenbacher F 2002 *Phys. Rev. Lett.* **88** 156102
[6] Ertl G and Freund H-J 1999 *Phys. Today* **52** 32
[7] Antczak G and Ehrlich G 2004 *Phys. Rev. Lett.* **92** 166105
[8] Goergievskii Y and Pollak E 1994 *Phys. Rev.* E **49** 5098
[9] Goergievskii Y and Pollak E 1996 *Surf. Sci.* **355** L 366
[10] Hershkovitz E, Talkner P, Pollak E and Goergievskii Y 1999 *Surf. Sci.* **421** 73
[11] Hänggi P, Talkner P and Borkovec M 1990 *Rev. Mod. Phys.* **62** 251
[12] Sancho J M, Lacasta A M, Lindenberg K, Sokolov I M and Romero A H 2004 *Phys. Rev. Lett.* **92** 250601
Sancho J M, Lacasta A M, Lindenberg K, Sokolov I M and Romero A H 2004 *Phys. Rev.* E, at press (*Preprint* cond-mat/0407781)
[13] Barone G and Paterno A 1982 *Physics and Applications of the Josephson Effect* (New York: Wiley)
[14] Kautz R L 1996 *Rep. Prog. Phys.* **59** 935
[15] Dieterich W, Fule P and Peschel I 1980 *Adv. Phys.* **29** 527
[16] Frenken J W M and Van der Veen J F 1985 *Phys. Rev. Lett.* **54** 34
Pluis B *et al* 1987 *Phys. Rev. Lett.* **59** 2678
Hershkovitz E, Talkner P, Pollak E and Georgevskii Y 1999 *Surf. Sci.* **421** 73
[17] Korda P T, Taylor M B and Grier D G 2002 *Phys. Rev. Lett.* **89** 128301
Gopinathan A and Grier D G 2004 *Phys. Rev. Lett.* **92** 130602
[18] Nixon G I and Slater G W 1996 *Phys. Rev.* E **53** 4969
[19] Risken H 1989 *The Fokker–Planck Equation* (Berlin: Springer) ch 11
[20] Borromeo M and Marchesoni F 2000 *Surf. Sci.* **465** L771
[21] Costantini G and Marchesoni F 1999 *Europhys. Lett.* **48** 491
[22] Reimann P *et al* 2001 *Phys. Rev. Lett.* **87** 010602
Reiman P *et al* 2002 *Phys. Rev.* E **65** 031104
[23] Heinsalu E, Tammelo R and Örg T 2004 *Phys. Rev.* E **69** 021111
[24] Hayashi K and Sas S 2004 *Phys. Rev.* E **69** 066119
[25] Tatarkova S A, Sibbett W and Dholakia K 2003 *Phys. Rev. Lett.* **91** 038101
[26] Marchesoni F 1997 *Phys. Lett.* A **231** 61
[27] Shushin A I 2002 *Europhys. Lett.* **60** 525
[28] Gang U, Daffertshofer A and Haken H 1996 *Phys. Rev. Lett.* **76** 4874
[29] Schreier M, Reimann P, Hänggi P and Pollak E 1998 *Europhys. Lett.* **44** 416
[30] Coffey W T, Déjardin J L and Kalmykov Y P 2000 *Phys. Rev.* E **61** 4599
[31] Kallunki J, Dubé M and Ala–Nissila T 2000 *Surf. Sci.* **460** 39
[32] Lacasta A M, Sancho J M, Romero A H and Lindenberg K 2004, in preparation
[33] Lindner B, Kostur M and Schimansky-Geier L 2001 *Fluct. Noise Lett.* **1** R25
[34] Colet P, San Miguel M, Casademunt J and Sancho J M 1989 *Phys. Rev.* A **39** 149